and extends the findings of Saito et al.[5] and suggests that this is a general property of all GT steps. Recent observations have demonstrated that the cleavage resulting from 4′-hydrogen abstraction at GT steps occurs most frequently as part of a staggered double-strand break.[23] Additional studies using oligomers to explore the effects of thiols on the partitioning between 4′- and 5′-hydrogen abstraction and on the reduction of peroxide intermediates are in progress.

Acknowledgment. This research was supported by the National Institutes of Health GM 34454 (J.W.K. and J.S.) and National Institutes of Health CA 44257 and GM 12573 (I.H.G.).

(23) Dedon, P. C.; Goldberg, I. H. *J. Biol. Chem.* **1990**, *265*, 14713–14716.

Topographic Design of Peptide Neurotransmitters and Hormones on Stable Backbone Templates: Relation of Conformation and Dynamics to Bioactivity[1]

Wieslaw M. Kazmierski,[2a] Henry I. Yamamura,[2b] and Victor J. Hruby*[,2a]

Contribution from the Departments of Chemistry and Pharmacology, University of Arizona, Tucson, Arizona 85721. *Received June 4, 1990*

Abstract: We have proposed that development of methods for controlling the side-chain topography of amino acid residues in peptides and proteins provides a new approach to the topographical design of biologically active peptides. An example of this approach is the use of the 1,2,3,4-tetrahydroisoquinolinecarboxylic acid (Tic) residue, which favors a gauche (−) side-chain conformation when in the N-terminal position, whereas in its acylated form (internal position), the most stable side-chain conformation is gauche (+). This approach has been tested by incorporating D-Tic or Tic at different positions of μ opioid receptor specific octapeptides such as D-Phe-Cys-Tyr-D-Trp-Lys-Thr-Pen-Thr-NH_2 (CTP, **1**), examination of the biological consequences of these modifications, and detailed ^1H NMR based conformational analysis. The compounds prepared and their biological activities were as follows: D-Tic-Cys-Tyr-D-Trp-Lys-Thr-Pen-Thr-NH_2 (**2**; gauche (−), δ/μ = 7800, IC_{50} μ = 1.2 nM); Gly-D-Tic-Cys-Tyr-D-Trp-Orn-Thr-Pen-Thr-NH_2 (**3**; gauche (+), δ/μ = 19, IC_{50} μ = 278.7 nM); and D-Phe-Cys-Tic-D-Trp-Orn-Thr-Pen-Thr-NH_2 (**4**; gauche (+), δ/μ = ~7, IC_{50} μ = 1439.0 nM). In the absence of a geminal pair of protons suitable for distance calibration, a new technique (Davis, D. G. *J. Am. Chem. Soc.* **1987**, *109*, 3471–3472) of transverse and longitudinal cross-relaxation rate measurements has been utilized in conjunction with other 2D NMR methods in order to determine the three-dimensional solution conformations for the peptides **1–4**, with subsequent application of restrained molecular dynamics (GROMOS). The average backbone conformations in peptides **1–4** were very similar, but the side-chain conformational preferences in the analogues differed, suggesting that the different affinities and selectivities for μ opioid receptors were primarily due to differences in the side-chain conformations of Tic (D-Tic), and thus due to differences in the topographies of these peptides, and not the backbone conformations. A detailed analysis of these relationships is presented.

Introduction

A dogma in molecular biology is that the biological function ("function" code) of biologically active peptides is determined by the conformations coded in their primary structure ("structure" code). For peptide neurotransmitters and hormones, transfer of their biological messages to the target cells via specific receptors requires at least two consecutive events: (1) binding of the hormone or neurotransmitter to its receptor; (2) transduction of the information from the hormone–receptor complex into the cell, leading to a biological response.[3] Since the structural, conformational, and dynamic properties of the peptide hormone and its receptor play a key role in both steps, their recognition and control are essential prerequisites to understanding the molecular basis of information transfer in these systems. In principle, the most direct approach would be the use of transferred nuclear Overhauser effect (TRNOE) studies of the neurotransmitter bound to its receptor. This method has provided insights into the conformations of small ligands bound to proteins.[4-6] Currently there are no isolated opioid receptors available. However, in principle this goal also may be pursued by examination of the conformational and dynamic properties of constrained synthetic hormone analogues carefully selected for their complementary biological properties.

Opioid peptides, owing to the multiplicity of opioid receptors, display a variety of biological actions. At least four major classes of opioid receptors have been postulated so far; μ, δ, κ, and ϵ. Recognition of the conformational and dynamic features of ligands

(1) Preliminary communication of this work was presented in part during the 10th American Peptide Symposium, May 23–28, 1987, St. Louis, MO, and the 13th International Conference on Magnetic Resonance in Biological Systems, Madison, WI, August 14–19, 1988. Symbols and abbreviations are in accord with the recommendations of the IUPAC–IUB Commission on Biochemical Nomenclature (*J. Biol. Chem.* **1972**, *247*, 977). All optically active amino acids are of the L variety unless otherwise stated. Other abbreviations include the following: Tic, 1, 2, 3, 4-tetrahydroisoquinolinecarboxylic acid; Pen, penicillamine or β,β-dimethylcysteine; Orn, ornithine; TRNOE, transferred nuclear Overhauser effect; NOE, nuclear Overhauser effect; DIEA, diisopropylethylamine; *p*-MBHA, *p*-methylbenhydrylamine; TPPI, time-proportional phase increments; CTP, D-Phe-Cys-Tyr-D-Trp-Lys-Thr-Pen-Thr-NH_2; CTOP, D-Phe-Cys-Tyr-D-Trp-Orn-Thr-Pen-Thr-NH_2-N^{α}-*tert*-butyloxycarbonyl; Cbz, benzyloxycarbonyl; GPI, guinea pig ileum; MVD, mouse vas deference.

(2) (a) Department of Chemistry. (b) Department of Pharmacology.

(3) Hruby, V. J. In *Perspectives in Peptide Chemistry: Structure, Conformation and Activity*; Eberle, A., Geiger, R., Wieland, T., Eds.; Karger: Basel, Switzerland, **1981**, pp 207–220.

(4) Clore, G. M.; Gronenborn, A. M. *J. Magn. Reson.* **1982**, *48*, 402–417.

(5) Andersen, N. H.; Eaton, H. L.; Nguyen, K. T. *Magn. Reson. Chem.* **1987**, *25*, 1025–1034.

(6) Hallenga, K.; Nirmala, N. R.; Smith, D. D.; Hruby, V. J. In *Peptides: Chemistry and Biology*, Proceedings of the Tenth American Peptide Symposium; Marshall, G. R., Ed., ESCOM: Leiden, The Netherlands, 1988; pp 39–41.

0002-7863/91/1513-2275$02.50/0

Table I. Binding Affinites of Peptides **1–4** in Competition with [^{3}H]CTOP[a] and [^{3}H]DPDPE[b] and Their Inhibitory Activity in the in Vivo Hot Plate Test[c]

peptide	IC_{50},[d] nM vs [^{3}H]CTOP	IC_{50},[d] nM vs [^{3}H]DPDPE	in vivo pA_2[b]
D-Phe-Cys-Tyr-D-Trp-Lys-Thr-Pen-Thr-NH_2 (**1**)	3.7 ± 0.8	1153 ± 116	11.17
D-Tic-Cys-Tyr-D-Trp-Lys-Thr-Pen-Thr-NH_2 (**2**)	1.2 ± 0.03	9324 ± 546	11.29
Gly-D-Tic-Cys-Tyr-D-Trp-Orn-Thr-Pen-Thr-NH_2 (**3**)	278.7 ± 0.5	5352 ± 503	ND
D-Phe-Cys-Tic-D-Trp-Orn-Thr-Pen-Thr-NH_2 (**4**)	1439.0 ± 215	>10000	ND

[a] μ opioid selective antagonis,[7] CTOP, D-Phe-Cys-Tyr-*D*-Trp-Orn-Thr-Pen-Thr-NH_2. [b] δ opioid selective agonist,[62] DPDPE, Tyr-*D*-Pen-Gly-Phe-*D*-Pen. [c] Percent in vito measurement of antagonist potency.[8] Rat brain binding assays. ND, not determined due to low antagonist potency. [d] IC_{50}, inhibitory concentration at which 50% of a receptor-bound radioligand is displaced by a ligand (agonist or antagonist) under investigation. [e] pA_2 refers to the −log of the concentration of inhibitor requiring twice the concentration of agonist (e.g., morphine) to induce its original biological response.

selective for only one of them may provide important insights into the basis of molecular recognition and information transfer in the opioid receptor system. We have synthesized and biologically evaluated a number of peptide μ receptor antagonists from which four have been selected for further conformational studies due to their interesting structures and μ opioid receptor potency and selectivity relationships (Table I).

Replacement of the D-Phe[1] in D-Phe-Cys-Tyr-D-Trp-Lys-Thr-Pen-Thr-NH_2 (**1**, CTP) by a D-tetrahydroisoquinoline-carboxylic acid (D-Tic) residue resulted in an analogue (**2**) with a substantial increase in selectivity and affinity for the μ opioid receptor.[7,8] On the other hand, attachment of Gly to the N terminal of peptide **2** (analogue **3**), resulted[8] in a dramatic decrease of potency and selectivity for the μ opioid receptor. Similarly, substitution of Tyr[3] by Tic[3], as in peptide **4**, decreases its potency at μ opioid receptors. These results became even more intriguing, in light of our preliminary findings[9] that all of those peptides exhibited very similar backbone conformations. Thus, we have investigated the conformational and topographical properties of these peptides in greater detail.

A useful tool in this approach is the determination of the interproton distances in peptides and proteins as measured by the nuclear Overhauser effect,[10] providing that the molecule contains a pair of geminal protons that can serve as a calibration standard of the interproton distance and magnitude of the Overhauser effect. Generally, α-protons of Gly, or δ-CH_2 protons of Pro are used for this purpose. Since these are not present (except in **3**) in peptides **1–4**, the β-CH_2 protons of other amino acids (e.g., D-Trp, Tyr, Orn, etc.) might be considered. However, it has been shown in several laboratories[11-13] that there is a nonnegligible effect of internal molecular motions on cross-relaxation for these protons both in laboratory and rotating frames. In practical terms, the presence of fast internal motions can alter (usually increase) the calculated interproton distances on the basis of NOE effects up to 20%.

While this may not constitute a problem for proteins, which usually have hundreds of observable NOEs that can be used in conjunction with distance geometry routines to provide averaged and self-consistent conformations, it is of considerable concern in the case of small peptides, which usually possess much fewer observable NOEs.

Recently, Davis[14] and Mirau and Bovey[15] have suggested NMR experiments capable of determining internuclear distances as well as correlation times (τ_c) for pairs of protons without any a priori assumptions about their internal motions.

The method of Davis involves measurements of longitudinal ($\sigma_\parallel$) and transverse ($\sigma_\perp$) cross-relaxation rates and is based on the observation that $\sigma_\parallel$ and $\sigma_\perp$ have different dependencies on τ_c (eqs 1 and 2). The ratio $R = \sigma_\parallel/\sigma_\perp$ is r_{AB} independent and

$$(\sigma_\perp)_{AB} = (\gamma^4\hbar^2/10r^6_{AB})(3/(1 + \omega^2_0\tau^2_c) + 2)\tau_c \quad (1)$$

$$(\sigma_\parallel)_{AB} = (\gamma^4\hbar^2/10r^6_{AB})(6/(1 + 4\omega^2_0\tau^2_c) - 1)\tau_c \quad (2)$$

gives an entry into τ_c correlations times between pairs of protons AB, whereas r_{AB} can be calculated from either eq 1 or eq 2, providing that τ_c is calculated for a given pair of protons (eq 3).

$$\tau_c^2 = \frac{-(1 - 22R) - [(1 - 22R)^2 + 80(1 + 2R)(1 - R)]^{1/2}}{-8(1 + 2R)\omega^2_0} \quad (3)$$

In this article, we will examine the utility of this novel approach for studies of the conformation and dynamics of the 20-membered rings of the cyclic octapeptides **1–4**. We will then correlate the stereochemical (r_{AB}) and dynamic (τ_c) features determined with the observed activities and selectivities for μ opioid receptors for these peptides and postulate those structural elements that are responsible for the high degree of molecular recognition for ligand–μ opioid receptor interactions. Finally, the applicability of tetrahydroisoquinoline-carboxylic acid (Tic) to protein/peptide design will be discussed.

Experimental Section

Materials and Methods. The synthesis and biological properties of peptides **1–3** have already been reported.[7,8] Compound **4** was synthesized according to published methods[7,8] using solid-phase synthesis techniques[16,17] with a Vega (Tucson, AZ) Model 250 peptide synthesizer. Amino aicds either were purchased from Bachem (Torrance, CA) or were prepared by literature methods.[16] The synthesis was accomplished on a *p*-methylbenzhydrylamine (*p*MBHA) resin[18] (substitution 1.0 mM/g of resin). A 1.5 M excess of preformed symmetrical anhydrides or 3 M excess of hydroxybenzotriazole active esters was used for coupling reactions, which were monitored by ninhydrin[19] or chloranil[20] tests. The protected peptide resin (1 mM) of **4** was synthesized by sequential coupling, deprotection with trifluoroacetic acid (TFA), and neutralization with diisopropylethylamine (*DIEA*) of N^α-Boc-Thr(*O*-Bzl), N^α-Boc-Pen(*S*-4-MeBzl) (Pen, β,β-dimethylcysteine), N^α-Boc-Thr(*O*-Bzl), N^α-Boc-Orn(N^δ-Cbz), N^α-Boc-Tic, N^α-Boc-Cys(*S*-4-MeBzl), and N^α-Boc-D-Phe. After N^α-Boc-D-Trp was coupled, the deprotecting TFA solution (v/v/v; 48% TFA, 2% anisole, and 50% dichloromethane (DCM)), was modified to contain 48% TFA, 2% anisole, 10% dithioethane, 20% di-

(7) Pelton, J. T.; Kazmierski, W.; Gulya, K.; Yamamura, H. I.; Hruby, V. J. *J. Med. Chem.* **1986**, *29*, 2370–2375.
(8) Kazmierski, W.; Wire, W. S.; Lui, G. K.; Knapp, R. J.; Shook, J. E.; Burks, T. F.; Yamamura, H. I.; Hruby, V. J. *J. Med. Chem.* **1988**, *31*, 2170–2177.
(9) Kazmierski, W.; Yamamura, H. I.; Burks, T. F.; Hruby, V. J. In *Peptides 1988*; Bayer, E., Young, G., Eds.; Walter de Gruyter & Co.: Berlin, 1989; pp 643–645.
(10) Noggle, J. H.; Schirmer, R. E. In *The Nuclear Overhauser Effect*; Academic Press: New York and London, 1971.
(11) (a) Lipari, G.; Szabo, A. *J. Am. Chem. Soc.* **1982**, *104*, 4546–4559. (b) Lipari, G.; Szabo, A. *J. Am. Chem. Soc.* **1982**, *104*, 4459–4570.
(12) Olejniczak, E. T.; Dobson, C. M.; Karplus, M.; Levy, R. M. *J. Am. Chem. Soc.* **1984**, *106*, 1923–1930.
(13) Farmer, B. T., II; Macura, S.; Brown, L. R. *J. Magn. Reson.* **1988**, *80*, 1–22.
(14) Davis, D. G. *J. Am. Chem. Soc.* **1987**, *109*, 3471–3472.
(15) Mirau, P. A.; Bovey, F. A. *J. Am. Chem. Soc.* **1986**, *108*, 5130–5134.
(16) Stewart, J. M.; Young, J. D. In *Solid Phase Peptide Synthesis*, 2nd ed.; Pierce Chemical Co.: Rockford, IL, 1984.
(17) Upson, D. A.; Hruby, V. J. *J. Org. Chem.* **1976**, *41*, 1353–1358.
(18) Orlowski, R. C.; Walter, R.; Winkler, D. *J. Org. Chem.* **1976**, *41*, 3702–3705.
(19) Keiser, E.; Colescott, R. L.; Bossinger, C. D.; Cook, P. I. *Anal. Biochem.* **1970**, *34*, 595–598.
(20) Christensen, T. In *Peptides, Structure and Biological Functions*; Gross, E., Meienhofer, J., Eds.; Pierce Chemical Co.: Rockford, IL, 1979; pp 385–388.

Table II. ^{1}H NMR Spectral Assignments (ppm) for the Aliphatic and Amide Resonances of Gly-D-Tic^1-Cys-Tyr^3-D-Trp-Orn-Thr-Pen-Thr-NH_2 (**3**) and D-Phe^1-Cys-Tic^3-D-Trp-Orn-Thr-Pen-Thr-NH_2 (**4**) in [$^2H_6$]DMSO, 303 K[a]

	residue	**3**	**4**
(**3**)	Gly^0 NH	8.02	
(**3**)	H α-CH_2	4.85/4.54 (J_9 = 15.4)	
(**3**)	residue 1 NH		8.06 (m)
(**4**)	α-CH	5.05 ($J_{\alpha\beta}$ = 6.3, 6.3)	4.02 ($J_{\alpha\beta}$ = 4.9, 9.5)
	β-CH	3.34 (J_9 = 15.4)	3.23 (J_9 = 13.8)
		3.13	2.96
	N-CH_2	4.57 (m)	
Cys^2	NH	8.63 (J = 9.8, $\Delta\delta/\Delta T$ = −4.7)	9.25 (J = 8.7, $\Delta\delta/\Delta T$ = −4.1)
	CH_α	5.37 ($J_{\alpha\beta}$ = 7.3, 3.7)	5.47 ($J_{\alpha\beta}$ = 4.6 10.0)
	CH_β	2.78 (J_9 = 15.4)	3.20 (J_9 = 13.6)
		2.68	2.92
(**3**)	residue 3 NH	8.56 (J = 7.8, $\Delta\delta/\Delta T$ = −4.1)	
(**4**)	residue 3 α-CH	4.55 ($J_{\alpha\beta}$ = 8.7, 6.1)	5.22
	β-CH	2.68	2.95 ($J_{\alpha\beta}$ = 4.1, 5.8)
			2.84 (J_9 = 15.8)
	N-CH_2		4.89 (m)
D-Trp^4	NH	8.87 (J = 5.4, $\Delta\delta/\Delta T$ = −4.0)	8.09 (J = 6.2, $\Delta\delta/\Delta T$ = −4.7)
	α-CH	4.15 ($J_{\alpha\beta}$ = 8.4, 7.3)	4.27 ($J_{\alpha\beta}$ = 6.6, 8.8)
	β-CH	3.00	3.04 (J_9 = 14.2)
		2.73	2.36
Orn^5	NH	8.33 (J = 9.3, $\Delta\delta/\Delta T$ = −2.7)	8.29 (J = 8.0, $\Delta\delta/\Delta T$ = −3.1)
	α-CH	4.09 ($J_{\alpha\beta}$ = 10.5, 3.2)	4.07 ($J_{\alpha\beta}$ = 4.7, 9.1)
	β-CH	1.85	1.70
		1.14	1.25
	γ-CH	0.92	1.18
	δ-CH	2.58	2.58
	δ-NH_3^+	7.58	
Thr^6	NH	7.65 (J = 9.1, $\Delta\delta/\Delta T$ = −0.2)	7.28 (J = 7.8, $\Delta\delta/\Delta T$ = −0.8)
	α-CH	4.58 ($J_{\alpha\beta}$ = 7.0)	4.39 ($J_{\alpha\beta}$ = 4.5)
	β-CH	3.92 (J_β = 6.5)	3.88 ($J_{\beta\gamma}$ = 6.3)
	γ-CH	1.05	0.91
Pen^7	NH	8.41 (J = 9.8, $\Delta\delta/\Delta T$ = −6.0)	7.92 (J = 9.0, $\Delta\delta/\Delta T$ = −2.0)
	α-CH	4.78	4.80
	γ-CH	1.17/0.90	1.27/1.40
Thr^8	NH	7.95 (J = 3.0, $\Delta\delta/\Delta T$ = −2.1)	8.32 (J = 8.3, $\Delta\delta/\Delta T$ = −4.4)
	α-CH	4.23 ($J_{\alpha\beta}$ = 3.9)	4.26 ($J_{\alpha\beta}$ = 3.9)
	β-CH	4.00 ($J_{\beta\gamma}$ = 6.3	4.01 ($J_{\beta\gamma}$ = 6.4)
	γ-CH	0.99	1.05

[a] Coupling constants in hertz.

methyl sulfide and 20% dichloromethane. After the last amino acid was coupled, the N^α-Boc protecting group was removed, the amino acid neutralized with DIEA, and the peptide resin dried in vacuo. The resulting (H)-D-Phe-Cys(*S*-4-MeBzl)-Tic-D-Trp-Orn(Z)-Thr(*O*-Bzl)-Pen-(*S*-4-MeBzl)-Thr(*O*-Bzl)-resin was cleaved with 15 mL of liquid HF and of 1 mL of anisole at 0 °C. The product was washed with ethyl ether (3 × 20 mL) and extracted with 10% aqueous acetic acid (HOAc; 3 × 20 mL) followed by glacial HOAc (2 × 20 mL), and both fractions were lyophilized separately. The linear peptide was cyclized by dissolving the lyophilized powder in 1.5 L of water (pH adjusted with aqueous ammonia to 8.5) followed by oxidation with 0.01 M aqueous $K_3Fe(CN)_6$ until the yellow color persisted for 20 min. After the reaction was terminated, the pH was adjusted to 4.5 with AcOH, and excess ferro- and ferricyanides were removed by 15 mL of Amberlite IRA-45 (mesh 15–60, Cl^- form). The mixture was stirred for 1 h and filtered, and the solution was concentrated in vacuo and lyophilized. Gel filtration on 100 × 2.5 cm Sephadex G-15 with 5% (v/v) aqueous HOAc was followed by reverse-phase HPLC with a gradient of 10–30% acetonitrile and 0.1% aqueous TFA on a Vydac C_{18} column: total yield 18.9%; FAB-MS $[M + H]_{calc}$ 1058, $[M + H]_{obs}$ 1058. The structure was confirmed additionally with ^{1}H NMR spectroscopy (Table II). Purity was assessed by thin-layer chromatography in three solvent systems and RP-HPLC.

Boc-Tic was obtained analogously to Boc-D-Tic[8] in 71.3% yield for the first step (Pictet–Spengler reaction), and a 94% yield for the N^α-Boc protection procedure.

Binding Studies. Binding studies were performed as described in previous reports.[7,8]

NMR Studies. The spectral assignments of peptides **1** and **2** in [$^2H_6$]DMSO were determined previously.[21,22] The ^{1}H NMR spectra of compounds **3** and **4** were acquired with a Bruker AM250 spectrometer equipped with an Aspect 3000 computer.

All samples (ca. 4–5 mg each) were dried overnight in vacuo, dissolved in [$^2H_6$]DMSO, degassed by repeated freeze–thaw cycles, and sealed. All the spectra were recorded at 20 °C, unless mentioned otherwise.

The phase-sensitive correlation experiments with double-quantum filter, using time-proportional phase increments (TPPI) were performed by methods described by Marion and Wüthrich[23] and Rance et al.[24] with 256 t_1 experiments and 64 scans of 1K data points. Multiplication by a shifted sine bell was applied in both dimensions. Zero filling in the t_1 dimension followed by Fourier transformation and phasing in both dimensions resulted in a final matrix of 1K × 1K points. Pulse sequence D1–90–D0–90–D3–90–FID.

Homonuclear shift-correlated 2D NMR experiments with a delay period to emphasize long-range or small couplings were run by the method of Bax and Freeman.[25] Pulse sequence D1–90–D0–D2–90–FID; D2 = 0.08 s; 256 t_1 experiments with 128 scans of 1K data points. Multiplication by a sine bell in both dimensions and zero filling in the t_1 dimension followed by Fourier transformation and phasing in both dimensions resulted in a final matrix of 1K × 1K.

Homonuclear dipolar correlated 2D NMR experiments in phase-sensitive mode using TPPI[26] were performed by acquisition of 256 t_1 experiments with 128 scans of 2K data points. Pulse sequence D1–90–D0–90–D9–90–FID. Zero-quantum scalar coupling correlations were suppressed by random variation (±20%) of the mixing time D9.

At least five experiments, with different mixing times ranging from 10 to 450 ms (represented on cross-relaxation buildup rate graphs) were run for each peptide investigated (**1–4**).

After acquisition, all data were transferred to a microVax 3200 for processing with the FTNMR program, version 5.1 (Hare Research, Inc.).

(21) Sugg, E. E.; Tourwe, D.; Kazmierski, W.; Hruby, V. J.; van Binst, G. *Int. J. Pept. Protein Res.* **1988**, *31*, 192–200.
(22) Kazmierski, W.; Hruby, V. J. *Tetrahedron* **1988**, *41*, 697–710.
(23) Marion, D.; Wüthrich, K. *Biochem. Biophys. Res. Commun.* **1983**, *113*, 967–974.
(24) Rance, M.; Sørensen, O. W.; Bodenhausen, G.; Wagner, R. R.; Ernst, R. R.; Wüthrich, K. *Biochm. Biophys. Res. Commun.* **1983**, *117*, 471–478.
(25) Bax, A.; Freeman, R. *J. Magn. Reson.* **1981**, *44*, 542–561.
(26) Bodenhausen, G.; Kogler, H.; Ernst, R. R. *J. Magn. Reson.* **1984**, *58*, 370–388.

Table III. Selected Longitudinal ($\sigma_{\parallel}$), Measured Transverse ($\sigma_{\perp}$ (exp ROE)), Corrected Transverse ($\sigma_{\perp}$)[a,b] Cross-Relaxation Rates, Correlation Times (τ_c),[c] Internuclear Distances (r^{ij}),[d] and Calculated Internuclear Distances (r^{ij}_{calc})[e] for D-Phe-Cys-Tyr-D-Trp-Lys-Thr-Pen-Thr-NH_2, (CTP, **1**), [D-Tic[1]]CTP (**2**), [Gly[0],D-Tic[1]]CTOP (**3**), and [Tic[3]]CTOP (**4**), in [$^2H_6$]DMSO, 303 K[f]

atom pair	$\sigma_{\parallel}$ (exp NOE)	$\sigma_{\perp}$ (exp ROE)	$\sigma_{\perp}$ (corr ROE)	τ_c^{ij}, ns	r^{ij}, Å	r_{calc}^{ij}, Å	atom pair	$\sigma_{\parallel}$ (exp NOE)	$\sigma_{\perp}$ (exp ROE)	$\sigma_{\perp}$ (corr ROE)	τ_c^{ij}, ns	r^{ij}, Å	r_{calc}^{ij}, Å
						Compound **1**							
α^1/NH^2	−0.69	4.10	4.37	1.01	1.8	2.1	$\alpha^5/\beta^5_{\parallel}$	0.0	0.26	0.27	0.71	2.8	2.8
α^2/NH^3	−0.26	3.30	3.30	0.84	1.9	2.2	$\alpha^7/\gamma^7_{\parallel}$	0.0	0.08	0.81	0.71	3.4	
α^3/NH^4	−0.78	4.31	4.62	1.03	1.8	2.5	NH^5/NH^6	−0.33	4.16	4.28	0.84	1.8	3.2
α^4/NH^5	−0.99	7.46	7.82	0.93	1.7	2.3	β^4/NH^4	−0.11	1.23	1.32	0.84	2.2	3.0
α^5/NH^6	−0.27	1.62	1.64	1.02	2.2	3.2	$\beta^4_{\parallel}/NH^4$	−0.28	1.84	2.0	0.96	2.1	
α^6/NH^7	−0.57	3.13	3.31	1.04	1.9	2.4	$\beta^5_{\parallel}/NH^5$	0.0	0.33	0.34	0.71	2.7	2.1
α^7/NH^8	−1.17	4.96	4.99	1.22	1.8	2.3	β^6/NH^6	−0.09	0.24	0.24	0.76	2.9	3.4
α^2/α^7	−0.67	2.67	2.67	1.28	2.0	2.2	β^6/NH^7	0.0	0.73	0.77	0.71	2.4	4.3
$\alpha^1/\beta^1_{/}$	0.0	0.61	0.62	0.71	2.5	2.5	β^6/NH^8	0.0	0.81	0.82	0.71	2.3	3.7
$\alpha^3/\beta^3_{/}$	0.0	0.61	0.64	0.71	2.4	2.7	$\beta^1_{\parallel}/NH^2$	0.0	0.02	0.02	0.71	4.2	
$\alpha^4/\beta^4_{\parallel}$	0.0	0.33	0.34	0.71	2.7	2.8	$\beta^1_{/}/NH^2$	0.0	0.69	0.75	0.71	2.4	
$\alpha^5/\beta^5_{\parallel}$	0.0	0.73	0.74	0.71	2.4	2.7							
						Compound **2**							
α^1/NH^2	−0.24	2.32	2.55	0.86	2.0	2.9	$\alpha^5/\beta^5_{\parallel}$	0.0	0.51	0.52	0.71	2.5	2.6
α^2/NH^3	−0.33	3.24	3.63	0.86	1.9	2.0	NH^5/NH^6	−0.40	1.39	1.40	1.36	2.3	4.2
α^3/NH^4	−0.72	4.88	5.23	0.96	1.8	2.0	$\beta^4_{\parallel}/NH^4$	0.0	0.56	0.60	0.71	2.5	3.2
α^4/NH^5	−0.41	8.93	9.14	0.78	1.6	1.7	$\beta^4_{\parallel}/NH^4$	0.0	1.25	1.34	0.71	2.2	1.9
α^5/NH^6	−0.16	3.47	3.54	0.78	1.9	3.6	$\beta^5_{\parallel}/NH^5$	0.0	0.53	0.56	0.71	2.5	2.5
α^6/NH^7	−0.39	4.43	4.68	0.85	1.8	2.5	$\beta^5_{\parallel}/NH^5$	not					
α^7/NH^8	−0.52	2.91	2.93	1.05	2.0	3.4		observed					
α^2/α^7	−0.43	3.71	3.71	0.91	1.9	1.8	β^6/NH^7	0.0	0.82	0.87	0.71	2.3	4.3
$\alpha^5/\beta^5_{/}$	0.0	0.35	0.35	0.71	2.7	2.7	$\beta^3_{/}/NH^3$	0.0	0.63	0.67	0.71	2.4	3.5
						Compound **3**							
α^1/NH^2	−0.20	3.27	3.47	0.80	1.9	2.2	$\alpha^4/\beta^4_{\parallel}$	−0.05	0.95	1.1	0.79	2.3	2.2
α^2/NH^3	−0.29	2.30	2.43	0.92	2.0	2.0	$\alpha^2/\beta^2_{\parallel}$	−0.05	0.68	0.68	0.84	2.5	2.4
α^3/NH^4	−0.61	4.02	4.31	0.96	1.8	2.4	α^7/β^6	0.0	0.50	0.50	0.71	2.5	4.9
α^4/NH^5	−0.63	3.25	3.42	1.07	1.9	1.7	α^7/β^8	0.0	1.07	1.08	0.71	2.2	5.0
α^5/NH^6	−0.02	1.76	1.79	0.73	2.1	3.7	NH^5/NH^6	−0.28	1.61	1.70	1.03	2.2	3.0
α^6/NH^7	−0.48	3.78	3.98	0.92	1.8	2.4	$\beta^5_{/}/NH^5$	0.0	0.09	0.10	0.71	3.3	2.9
α^7/NH^8	−0.26	3.80	3.94	0.82	1.8	2.1	$\beta^4_{/}/NH^4$	0.0	0.55	0.59	0.71	2.5	2.1
$\alpha^0_{/}/NH^3$	0.0	0.12	0.13	0.71	3.2		$\beta^4_{\parallel}/NH^4$	0.0	1.48	1.58	0.71	2.1	3.3
α^2/α^7	−0.54	3.78	3.78	0.97	1.9	2.1	β^6/NH^6	−0.08	3.65	3.75	0.74	1.8	3.2
$\alpha^1/\beta^1_{\parallel}$	−0.02	0.67	0.70	0.76	2.4		β^6/NH^7	0.0	1.26	1.32	0.71	2.2	4.2
$\alpha^0_{/}/\beta^6$	0.0	0.36	0.36	0.71	2.7		β^8/NH^6	0.0	1.77	1.80	0.71	2.1	
						Compound **4**							
α^1/NH^2	−0.54	2.96	3.24	1.03	1.9	2.6	$\beta^2_{/}/\alpha^7$	0.0	0.56	0.56	0.71	2.5	4.6
α^3/NH^4	−0.32	2.67	2.68	0.92	2.0	2.4	α^4/β^4	0.0	0.11	0.11	0.71	3.3	2.7
α^4/NH^5	−0.13	3.08	3.12	0.77	1.9	2.4	NH^5/NH^6	−0.05	1.34	1.40	0.76	2.2	4.2
α^6/NH^7	−0.20	1.81	1.88	0.89	2.1	2.1	$\gamma^7_{\parallel}/NH^7$	0.0	1.37	1.42	0.71	2.1	
α^7/NH^8	−0.12	1.34	1.35	0.85	2.2	3.4	$\beta^4_{/}/NH^4$	0.0	1.98	2.06	0.71	2.0	2.1
α^2/α^7	−0.08	0.82	0.82	0.87	2.4	1.9	$\beta^4_{\parallel}/NH^4$	0.0	0.53	0.56	0.71	2.5	3.1
$\beta^2_{\parallel}/\alpha^2$	0.0	0.94	0.94	0.71	2.3		$\beta^5_{/}/NH^5$	0.0	0.0				
$\beta^2_{\parallel}/\alpha^2$	0.0	0.50	0.50	0.71	2.5	2.5	β^6/NH^7	0.0	0.31	0.32	0.71	2.7	4.4
$\beta^2_{/}/\alpha^2$	0.0	0.23	0.23	0.71	2.9	1.6	$\beta^2_{\parallel}/NH^2$	0.0	0.65	0.71	0.71	2.4	3.1
$\beta^2_{\parallel}/\alpha^7$	0.0	1.30	1.30	0.71	2.2	4.3	$\beta^2_{/}/NH^2$	0.0	0.52	0.51	0.71	2.5	3.3

[a] In recriprocal seconds. [b] Calculated from eq 6. [c] Calculated from eq 3. [d] Calculated from eq 1. [e] Calculated by using GROMOS with r^{ij} distance constrains. [f] The rf carrier was positioned at 5.67 ppm, γB_{SL} = 3030 Hz. Offsets can be calculated by using data in Table II for **3** and **4** (see ref 21 for **1** and ref 22 for **2**). $\beta_{/}$, $\gamma_{/}$ refer to downfield diastereotopic protons. $\beta_{\parallel}$, $\gamma_{\parallel}$ refer to upfield diastereotopic protons.

The 1K complex point FIDs (2K by Bruker nomenclature) were multiplied by a shifted (π/2) sine-bell function extending to 1024 points in F2 and to 256 points in F1 dimensions, followed by zero filling in the F1 dimension. Fourier transformation and phase correction in both dimensions resulted in a 1K × 1K matrix.

$$D1 = 1.5\ s \qquad D0 = 3 \times 10^{-6}$$

The homonuclear dipolar correlated spectroscopy experiments in a rotating frame (CAMELSPIN, ROESY) were performed utilizing principles described by Bothner-By[27] and Bax and Davis,[28] in a phase-sensitive mode using TPPI; pulse sequence D1–90–D0–SL–FID. The spin-lock field, which used γB_{SL} = 3030 Hz, was generated by a low-power transmitter. At least five experiments for each peptide **1**–**4** with different spin-lock times ranging from 0.01 to 0.15s (presented on cross relaxation in the rotating-frame buildup rate graphs—see text) were made.

After acquisition of 256 t_1 experiments with 32 scans of 2K data points, the data were transferred and processed analogously to the procedure outlined for 2D NOE spectra.

In each of the 2D NOE and 2D ROE experiments the measurements of cross-peak and corresponding diagonal-peak volumes were carried out by defining an oval around each peak and volume integration routine provided by FTNMR. For each given experiment the cross-peak volumes were scaled according to a procedure suggested by Macura et al.,[29] eq 4, where τ_m is the mixing (NOE) or spin-lock time (ROE), a_{AB} is the

$$a_2(\tau_m) = \frac{a_{AB}(\tau_m)}{(1/2)n_B a_{AA}(\tau_m) + (1/2)n_A a_{BB}(\tau_m)} \qquad (4)$$

cross-peak intensity, a_{AA} is the diagonal-peak intensity, a_{BB} is the diagonal-peak intensity, n_A is the number of equivalent atoms A, and n_B is the number of equivalent atoms B.

This methodology allows for corrections of any variations between experiments (number of scans, signal/noise ratio, etc.), and most of all, $a_2(\tau_m)$ is a monotonically increasing function that is linear over a wider range with respect to either spin-lock or mixing times than the absolute cross-peak volumes are.

If both diagonal peaks (AA and BB) are not resolved well enough for integration, the cross–diagonal peak volumes are scaled with regard to

(27) Bothner-By, A. A.; Stephens, R. L.; Lee, J.; Warren, C. D.; Jeanloz, R. W. *J. Am. Chem. Soc.* **1984**, *106*, 811–813.
(28) Bax, A.; Davis, D. G. *J. Magn. Reson.* **1985**, *63*, 565–569.
(29) Macura, S.; Farmer, B. T., II; Brown, L. R. *J. Magn. Reson.* **1986**, *70*, 493–499.

only one of them[29] (eq 5). In this work, eq 5 was used, even if resolution

$$a_1(\tau_m) = a_{AB}(\tau_m)/n_A a_{BB}(\tau_m) \quad (5)$$

of both diagonal peaks was good enough for integration purposes, and only the statistically better of the two values (with regard to A and B) was selected for further computations.

The linear regression and statistical data analysis were performed (Lotus Development Corp., release 2.01) for all the 2D-NOE and 2D-ROE experiments and selected values (see supplementary material for complete sets) are presented in Table III for peptides **1–4**, respectively. Transverse cross-relaxation is observed in the rotating frame with the spins oriented along an effective spin-locking field $\omega_e = \gamma B_{eff} = \gamma(\Delta^2 + B_{SL}^2)^{1/2}$ makes an angle $\beta = \sin^{-1}(B_{SL}/B_{eff})$ with the longitudinal component Δ in the rotating frame.[14] Therefore a 2-fold correction of these offset effects has to be made.

Since the intensity of the ROE cross-peak between spins A and B is proportional to $\sin \beta_A \times \sin \beta_B$, while the intensity of the diagonal peaks is proportional to $\sin^2 \beta_A$ and $\sin^2 \beta_B$ for spins A and B, respectively, the cross-relaxation rate $a_2(\tau_{SL})$ or $a_1(\tau_{SL})$ must be corrected by a factor of $\sin \beta_A/\sin \beta_B$ if the cross-peak was normalized relative to B diagonal peak, or by $\sin \beta_B/\sin \beta_A$ if the cross-peak was referenced (eq 5) relative to an A diagonal peak.[30]

Another correction is necessary based on the observation that the measured transverse cross-relaxation rate contains a component of longitudinal cross-relaxation,[14] eq 6, where σ_{RF} is the experimental

$$(\sigma_{RF})_{AB} = \cos \beta_A \cos \beta_B(\delta_{\parallel})_{AB} + \sin \beta_A \sin \beta_B(\sigma_{\perp})_{AB} + (\gamma^4\hbar^2/10r^6_{AB}) \sin^2 \beta_A \sin^2\beta_B[(1 + 4\omega_e\tau_c^2)^{-1} - 1]\tau_c \quad (6)$$

transverse cross-relaxation rate, $\sigma_{\parallel}$ is the longitudinal transverse cross-relaxation rate, τ_c is the correlation time, and r_{AB} is the internuclear distance between protons A and B.

Since in solution $\omega_e^2\tau_c \ll 1$, the last term in eq 6 may be omitted, and the pure transverse cross-relaxation rates $\sigma_{\perp}$ calculated (Table III and supplementary material).

The assignment of prochiral β-methylene protons was carried out as described by Sørensen et al.[31] This method makes use of both $J_{\alpha\text{-NH}}$ coupling constant and magnitude of $NH/\beta_{\parallel}$ and $NH/\beta_{\parallel}$ dipolar relaxation (NOE, ROE), as well as simple geometrical consideration to deduce stereospecific response assignments of both diastereotopic β-protons.

Distance Geometry Calculations. Restrained molecular dynamics (MD) and energy minimization (EM) calculations were performed with the program from the Groningen Molecular Simulation (GROMOS) software package, made available to us by Drs. W. F. van Gunsteren and H. T. C. Berendsen (University of Groningen, Groningen, The Netherlands).[32-34]

The empirical potential energy function describing the interatomic interactions contains terms representing covalent bond stretching, bond angle bending, harmonic dihedral angle bending (improper dihedral for out-of-plane and out-of-tetrahedral configurations), and dihedral torsions, as well as Coulombic and van der Waals interactions. In addition, both an attractive and a repulsive distance restraint potential were applied to force the molecule to satisfy NOE distances determined in this work.

For an attractive distance restraint, the potential is represented by eq 7.

$$\begin{aligned} V_{dc}(r_{nn'}; r^0_m) &= 0 \quad 0 < r_{nn'} < r^0_m \\ &= \tfrac{1}{2}K^{dc}_m[r_{nn'} - r^0_m]^2 \quad r^0_m < \gamma_{nn'} < r^0_m + \Delta r^h \\ &= +K^{dc}_m[r_{nn'} - r^0_m - \tfrac{1}{2}\Delta r^h]\Delta r^h \quad r^0_m + \Delta r^h < r_{nn'} \end{aligned} \quad (7)$$

A repulsive distance restraint is represented by eq 8. The actual

$$\begin{aligned} V_{dc}(r_{nn'}; r^0_m) &= -K^{dc}_m[r_{nn'} - \gamma^0_m + \tfrac{1}{2}\Delta r^h]\Delta r^h \quad 0 < r_{nn'} < r^0_m - \Delta r^h \\ &= \tfrac{1}{2}K^{dc}_m[r_{nn'} - r^0_m]^2 \quad r^0_m - \Delta r^h < r_{nn} < r \\ &= 0 \quad r^0_m < r_{nn'} \end{aligned} \quad (8)$$

distance between atoms n and n' is denoted by $r_{nn'}$, and r^0_m represents a distance above which (or below which in the case of an attractive restraint) the potential is set to zero in a repulsive potential energy term. Δr^h represents the interatomic distance for which a quadratic potential is applied and has been set to 10 Å throughout all calculations. The value of restraining force constants CDIS was 9000 kJ/(mol nm^2), and the parameters for bonded and nonbonded interaction functions[35] were applied as given previously.

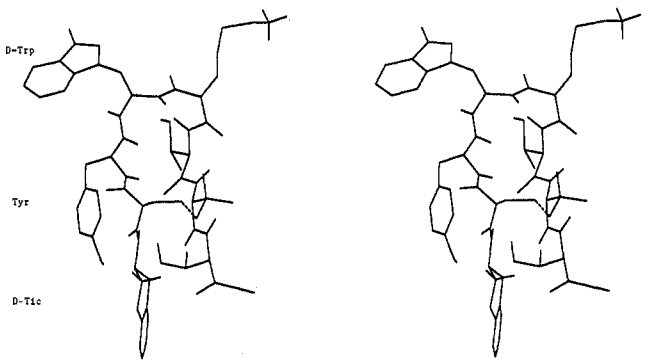

Figure 1. Stereoview of the conformation of D-Tic-Cys-Tyr-D-Trp-Lys-Thr-Pen-Thr-NH_2 (**2**), consistent with a type II′ β turn and negative disulfide chirality. The conformation was obtained after 20 ps of restrained MD, followed by EM (obtained with GROMOS software with NOE constraints K_{dc} = 9000, kJ/(nm^2 mol)). The conformations and restraints used were those in Table III and those found in the supplementary material.

Cutoff radii for nonbonded interactions for long-range Coulomb forces were set to 10 Å. While the united-atom approach is used in GROMOS, protons for which the NOE data were available were treated explicitly in the NOE potential energy terms. The NOE distance restraint atom pairs utilized in the dynamics studies are listed in Table III for peptides **1–4**, respectively. First, restricted EM (conjugate gradient[36]) to remove strains and bad contacts in the molecules **1–4** were run for each molecule. Second, restricted MD calculations were carried on for 20 ps with similar parameters as described. MD structures from the evolution period of the restrained molecular dynamics were averaged and repeatedly energy minimized (with use of NOE constraints) until energy converged, resulting in a final set of coordinates for peptides **1–4** that fulfilled the NOE requirements.

The resulting structures were examined with a MIDAS (Molecular Interactive Display and Simulation) software package running on Silicon Graphics IRIS 2000 system. A stereoview of the conformation for [D-Tic^1]CTP (**2**), is shown in Figure 1. Stereoviews for CTP (**1**), [Gly, D-Tic^1]CTOP (**3**) and [Tic^3]CTOP (**4**) are found in supplementary material.

Results

NMR Assignments. The strategy for determining the NMR resonance assignments for the peptides CTP (**1**) and [D-Tic^1]CTP (**2**) has been published already.[21,22] A similar approach was utilized for the spectral assignments for the peptides [Gly-D-Tic^1]CTOP (**3**) and [Tic^3]CTOP (**4**). These data are given in Table II. As previously observed for other compounds of this class,[21,22] there are two important NOEs between α-CH^4/NH^5 and NH^5/NH^6 for peptide **3**. The presence of these and the absence of other cross-relaxation effects suggest a type II′ β-turn backbone conformation for **3**.[37,38] This assumption identifies ϕ^{i+1}, ψ^{i+1} and ϕ^{i+2}, ψ^{i+2} as being in good conformity with those predicted for the ϕ angles by the $^3J_{\alpha\text{-NH}}$ coupling constants (Table II). The interresidual NOEs between α-CH^i and NH^{i+1} for **3** require a few comments. Strong cross-relaxation between α and amide protons (α^i–/NH^{i+1}) suggests that there are no cis peptide bonds present in **3** and also defines the possible range of ψ angles.[39] The

(30) Davis, D. G., private communication.
(31) Hengyi, S.; Ludvigsen, S.; Kjaer-Sørensen, D. W.; Poulsen, F. M. In Abstract book of the XIII International Conference on Magnetic Resonance in Biological Systems, Madison, WI, 1988; Poster P15-5.
(32) Berendsen, H. J. C.; van Gunsteren, W. F. In *Molecular Liquids. Dynamics and Interactions*; Barnes, A. J., et al. Eds.; NATO ASI Series C135; Reidel: Dordrecht, The Netherlands, 1984; pp 475–500.
(33) van Gunsteren, W. F.; Kaptein, R.; Zuiderweg, E. R. P. In *Proceedings of the NATO/CECAM Workshop on Nucleic Acid Conformations and Dynamics*; Olson, W. K., Ed.; Orsay, France, 1984; pp 73–92.
(34) Kaptein, R.; Zuiderweg, E. R. P.; Scheek, R. M.; Boelens, R.; van Gunsteren, W. F. *J. Mol. Biol.* **1985**, *182*, 179–182.
(35) Hermans, J.; Berendsen, H. J. C.; van Gunsteren, W. F.; Postma, J. P. M. *Biopolymers* **1984**, *23*, 1513–1518.
(36) McCammon, J. A.; Harvey, S. C. In *Dynamics of Protein and Nucleic Acids*; Cambridge University Press: New York, 1987.
(37) Kessler, H.; Berndt, M.; Kogler, H.; Zarbock, J.; Sørensen, O. W.; Bodenhausen, G. *J. Am. Chem. Soc.* **1983**, *105*, 6344–6952.
(38) Rao, B. N. N.; Kumar, A.; Balaram, H.; Ravi, A.; Balaram, P. *J. Am. Chem. Soc.* **1983**, *105*, 7423–7428.
(39) Wüthrich, K. *NMR of Proteins and Nucleic Acids*; Wiley: New York, 1986.

presence of an α-D-Tic/Cys NH cross-relaxation for **3** suggested a ψ_1 completely different from that found in **2**, possibly in the range of 180–300°. These interesting differences between the two compounds may be due to different side-chain conformations of the relatively rigid Tic residue. Another observation in comparison with **2**[22] is that the chemical shifts of the β-turn-forming residues are fairly comparable for both **2** and **3**, whereas some differences can be noticed for both the N- and C-terminal amino acid residues. Yet, the prominent cross-relaxation observed between the α-protons of Cys[2] and Pen[7] of **3** indicates that the disulfide helicity in peptide **3** is similar to that of peptide **2**. Focus of the analysis will now be directed toward the topography of the N-terminal residues in both **2** and **3**. As observed in Table II, both vicinal coupling constants of the D-Tic residue in **3** are equal and small and suggest a gauche (+) conformation of its side chain.

Interestingly, a huge (−0.81 ppm) upfield shift of Cys[2] NH is observed in **3** relative to **2**.[22] Similarly, though not as significant, an upfield shift was observed for the Thr[8] amide (−0.44). In light of earlier considerations, it is reasonable to suggest that these remarkable effects are due to anisotropic effects of the D-Tic ring. Furthermore, a very meaningful difference in the α-CH chemical shifts of tetrahydroisoquinoline residues in both **2** and **3** occurs (4.15 vs 5.05 ppm, respectively). In peptide **2** the gauche (−) conformation of χ_1 in Tic places the Tic α-CH proton in an axial position, leading to a weak upfield shift caused by the aromatic ring anisotropy. When the Tic conformation is gauche (+), as in **3**, the α-CH is in the deshielding cone of the aromatic ring and experiences a downfield shift relative to **2**.

Peptide **4** features a case of an internally incorporated Tic residue. Conformational analysis of **4** supports all the conclusions derived for peptide **3**. In addition, NOESY experiments reveal two important cross-peaks: Cys[2] α-CH/Tic[3] NCH_2 and Tic[3] α-CH/Tic[3] NCH_2. The first effect can only be observed if the corresponding peptide bond is in a trans configuration.[39] The 1D spectrum of **4** suggests that there is only one conformer observed. Thus, in contrast to the proline ring where cis and trans peptide bond isomers are often in equilibrium,[40–42] the tetrahydroisoquinoline ring seems to exclusively prefer a trans conformation of the peptide bond.[43]

The chemical shift difference between the diastereotopic methyl groups of Pen[7] was much larger in **4** (0.132 ppm) than in **1** (0.06 ppm). Table II reveals that there is a substantial upfield shift of the D-Trp[4] NH (−0.74 ppm in comparison to **1**[21]), which possibly is a result of ring anisotropy from the gauche (+) populated side chain of Tic, in contrast to the mostly gauche (−) populated side chain of Tyr in CTP (**1**).

Relaxation Studies. Table III (complete sets can be obtained in the supplementary material) presents selected longitudinal ($\sigma_\parallel$), and transverse ($\sigma_\perp$) cross-relaxation rates for proton pairs, for which correlation times and internuclear distances were calculated by using eqs 3 and 1, respectively. In majority of the cases a linear dependence of cross-relaxation rates on mixing time (NOE) or spin-lock time (ROE) was obtained in ranges up to 300 ms for NOE and 80 ms for ROE experiments (see supplementary material). Above these limits, nonlinearity effects are very pronounced due to spin diffussion,[44] and these experimental points are omitted in relaxation rate calculations.

Discussion

Most NMR-based conformational studies of peptides and proteins utilized quantitative nuclear Overhauser effects by scaling to its magnitude between a pair of geminal protons of either glycine or the δ-CH_2 protons of proline.[39,45] A major, though usually not discussed, assumption is that the molecule will tumble isotropically in solution, and that correlation times of all protons will be similar. The effect of molecular motions on cross-relaxation in the laboratory and rotating frames has been examined recently by Farmer et al.[13] Their results suggest that, for a molecule with varying degrees of internal motions, that kind of scaling may lead to erroneous results. In proteins, due to a large number of NOE cross-relaxations, these approximations are partially cancelled in the process of distance geometry calculations.[46] However, in small peptides, which usually have fewer NOEs per residue observable, the accuracy of internuclear distance measurement is of utmost importance. Since eqs 1 and 2 explicitly relate the magnitude of cross-relaxation in laboratory or rotating frames of reference, respectively, to the motion (τ_c), the strategy suggested by Davis[14] should be able to overcome this obstacle, should correlation times for various proton pairs differ significantly. It can be easily realized, upon inspection of Table III, that in peptides **1–4** the correlation time is rather conservative for the vast majority of proton pairs under consideration. Some of the proton pairs do exhibit cross-relaxation in a rotating frame, but only weak or no cross-relaxation in a laboratory frame of reference. This results in ratio of $\sigma_\parallel/\sigma_\perp = 0$, resulting in a trivial solution of eq 3, with $\tau_c = 0.71$ ns. For $\alpha\text{-CH}^i/\text{NH}^{i+1}$ pairs of protons, both transverse and longitudinal cross-relaxations can be detected, and calculated correlation times are in the range of 0.8–1.0 ns (α^7/NH^8 of **1**, $\tau_c = 1.2$ ns; α^7/NH^8 for **2**, $\tau_c = 1.1$ ns; α^4/NH^5 of **3** $\tau_c = 1.1$ ns). Comparing $\alpha\text{-CH}^i/\text{NH}^{i+1}$ distances derived from eq 1, one notices short distances for α^4/NH^5 for peptides **1** (1.7 Å) and **2** (1.6 Å), but not **3** (1.9 Å) and **4** (1.9 Å). While this variation for **4** may be related to the distorting effect of the neighboring cyclic side chain of Tic[3], the origin of that discrepancy for **3** is less apparent, but possibly is caused by different orientation of the side chain of D-Tic[1] (gauche (+)), compared to that of D-Phe[1] in **1** and D-Tic[1] in **2** (gauche (−)).

The transannular relaxation of Cys[2] α-CH/Pen[7] α-CH is also detectable in both frames of references with τ_c ranging from 0.9 (**2** and **4**) to 1.3 (**1**) ns. There is a measurable difference of the interproton distance for α^2/α^7 when peptides **1–3** (r = 1.9–2.0 Å) and **4** (r = 2.4 Å) are compared, which may be assigned to the presence of the rigid aromatic side chain of Tic[3] (in **4**), transannularly interacting with the disulfide bond.

Correlation times for NH^5/NH^6 differ somewhat among the analogues, being the shortest for **1** and **4** (0.8 ns), and longer for **3** (1.0 ns) and **2** (1.4 ns). Interestingly, the NH^5/NH^6 interproton distance for **4** differs somewhat from that of peptide **1** (2.2 vs 1.8 Å, respectively). The range of interproton distances for other pairs of nuclei (Table III) is quite broad and reaches as high as 4.2 ($\beta^1{}_\parallel/\text{NH}^2$ for **1**) and 3.44 Å ($\alpha^7/\gamma_\parallel{}^7$ for **1**).

Recently, Weaver et al.[47] analyzed the dynamics of a tryptophan side-chain group in two model peptides, *t*-Boc-LAWAL-OMe and *t*-Boc-LALALW-OMe in the absence as well as the presence of lysolecithin/D_2O micelles. While for the latter peptide τ_c for tryptophan side chains is ~15 times lower (0.07–0.09 ns) than the total correlation time (1.28 ns), both increase 10-fold in the presence of lysolecithin/D_2O micelles (0.9 to 1.1 and 14 ns, respectively). Though of a very qualitative nature, the comparison between the correlation times of side chains in *t*-Boc-LALALW-OMe and peptides **1–4** suggests that the presence of micelles, being a matrix for a linear, flexible peptide *t*-Boc-LALALW-OMe, excerts similar effects as cyclization in peptides **1–4** in terms of their dynamic properties.

Mirau and Bovey[15] investigated structural and dynamic properties of a poly(γ-benzyl-L-glutamate) (PBLG) by using nonselective and selective spin–lattice relaxation rates. Their results suggested that correlation times for NH and α-H are equal and

(40) Montelione, G. T.; Hughes, P.; Clardy, J.; Scheraga, H. A. *J. Am. Chem. Soc.* **1986**, *108*, 6765–6773.
(41) Piela, L.; Nemethy, G.; Scheraga, H. A. *J. Am. Chem. Soc.* **1987**, *109*, 4477–4485.
(42) Thomas, W. A. In *Annual Reports on NMR Spectroscopy*; Mooney, E. F., Ed.; Academic Press: New York, 1976; Vol. 6B.
(43) This conclusion may be valid for strained cyclic peptides. Our recent NMR studies of linear *p*-Br-Bz-Aib-D-Tic-AibOMe (one conformer), *p*-Br-Bz-$(Aib)_2$-Tic-$(Aib)_2$OMe (one conformer), and *p*-Br-Bz-Pro-D-TicNHMe (four conformers, 2 + 2) suggest this to be more complex problem: Kazmierski, W.; Toniolo, C.; Hruby, V. J., unpublished results.
(44) Kumar, A.; Wagner, G.; Ernst, R. R.; Wüthrich, K. *J. Am. Chem. Soc.* **1981**, *103*, 3654–3658.
(45) Bruch, M. D.; Noggle, J. H.; Gierasch, L. M. *J. Am. Chem. Soc.* **1985**, *107*, 1400–1407.
(46) Havel, T.; Wüthrich, K. *Bull. Math. Biol.* **1984**, *46*, 673–698.
(47) Weaver, A. J.; Kemple, M. D.; Prendegast, F. G. *Biophys. J.* **1988**, *54*, 1–15.

of a range expected for a rigid 20 amino acid helix (ca. 1.0 ns), whereas the β-H and γ-H protons showed internal motion relative to the overall tumbling (τ = 0.8 ns). Similarly, Niccolai et al.[48,49] found that in [D-Ala^2,Met^5]enkephalin, the τ_c for H^{δ}–H^{ϵ} vector of Tyr was only slightly faster than the one found for backbone protons showing that the aromatic ring is not freely rotating along the C^{δ}–C^{ϵ} axis of the tyrosine side chain.

Our results are, in a qualitative sense, strikingly similar to the above. While correlation times for side chains (α/β, etc.) are a little shorter (20–30%) than those characterizing backbone (and mostly originating from sequential α-CH^i/NH^{i+1}), this agrees well with a model of a cyclic peptide with a relatively rigid backbone conformation and slightly more floppy, but still rotationally restricted, side chains.

Distance Geometry Studies. Interatomic distances determined for atom points in peptides **1–4** were explicitly applied in restrained molecular dynamics calculations using the GROMOS methodology. The resulting structures for CTP(**1**), [D-Tic^1]CTP (**2**), [Gly-D-Tic^1]CTOP (**3**), and [Tic^3]CTOP (**4**) (see Figures 1 for **2**; stereoviews of **1**, **3**, and **4** are available in this supplementary material) reflect structures obtained from 20-ps restrained MD simulations. Due to the emphasis placed on the NOE constraining potential (large NOE force constant), however, they all incorporate experimental NOE distance constraints and as such provide useful models for the topographical design considerations to follow. Table III reveals selected internuclear distances in structures of peptides **1–4** obtained as a result of distance geometry calculations (a complete listing can be found in the supplementary material). In most cases the restraint violation is less than 0.5 Å, suggesting a good consistency between the resulting conformations and the restraining distances. The similarity of interproton distances for the various analogues (Table III) translated into distance geometry generated low-energy conformers for peptides **1–4** that readily incorporated all of the distance restraints. The conformations obtained can be visualized easily in Figure 1 for [[D-Tic^1]CTP (**2**) and for **1**, **3**, and **4** in supplementary material.

For CTP (**1**) the side-chain moieties of all three aromatic amino acids have some rotational freedom. However, the gauche (−) conformations are the most populated ones, positioning all three aromatic groups on one side of the molecule. This can be schematically represented by a Newman projection diagram of respective parts of the molecule (Figure 2A). The situation is very similar for [D-Tic^1]CTP (**2**) with all three aromatic groups on one side of the molecule (Figure 1). As a result of stabilization of a gauche (−) conformation in D-Tic^1, the all on one side arrangement is even more pronounced (Figure 1 and Newman projection Figure 3B). In the biological system this leads to an increase in μ vs δ opioid receptor potency and selectivity for **2** compared with **1** (Table I).

In [Gly^0, D-Tic^1]CTOP (**3**), as a result of a gauche (+) side-chain conformation for D-Tic^1, this aromatic ring is effectively rotated to the other side of the molecule (see Figure 2C for the Newman projection of a fragment tetrapeptide). This is accompanied by a dramatic decrease of affinity of peptide **3** for μ opioid receptors, suggesting that the N-terminal aromatic amino acid is an important binding element at the μ opioid receptor. An analogous effect may be observed for peptide **4**, [Tic^3]CTOP, which also weakly binds to μ opioid receptors. This can be correlated with an aromatic ring of Tic^3 rotated to the opposite side (with respect to D-Phe^1 and D-Trp^4) of the molecule as a result of a gauche (+) side-chain conformation (Figure 2D and supplementary material). Thus, the aromatic ring in the third position also appears to constitute a major pharmacaphore of μ opioid receptor selective ligands.

Conclusions

Most approaches in peptide/protein design to date have focused on an induction or stabilization of the backbone conformation.[50-52]

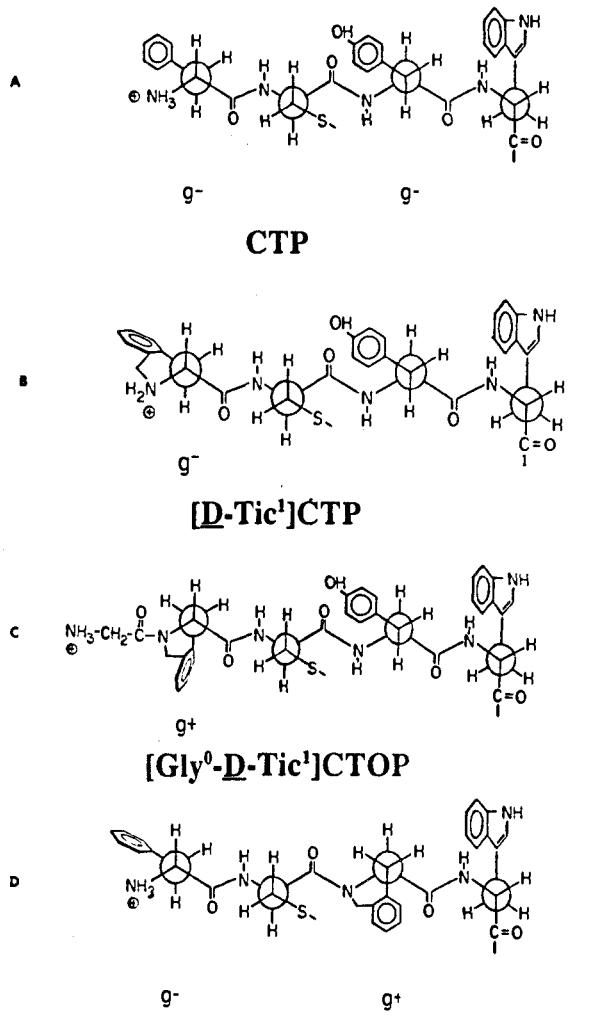

Figure 2. Newman representation of the aromatic ring topographies in peptides **1–4**. A. D-Phe-Cys-Tyr-D-Trp-Lys-Thr-Pen-Thr-NH_2 (**1**); B. D-Tic-Cys-Tyr-D-Trp-Lys-Thr-Pen-Thr-NH_2 (**2**); C. Gly-D-Tic-Cys-Tyr-D-Trp-Orn-Thr-Pen-Thr-NH_2 (**3**); D. D-Phe-Cys-Tic-D-Trp-Orn-Thr-Pen-Thr-NH_2 (**4**). g^- = gauche (**1**); g^+ = gauche (+). Only amino acid residues 1–4 are represented for simplicity. The side-chain conformation of 1,2,3,4-tetrahydroisoquinoline-3-carboxylate (Tic) is derived from $J_{\alpha\beta}$ coupling constants (Table II and refs 21 and 22).

Among these, template-assembled synthetic proteins,[53] use of sterically constrained α,α-dialkyl amino acids[54,55] and peptide mimetics[56-58] involving β turns and α helices and a variety of cyclization or ring-stabilizing strategies[50,51] have been proposed for secondary structure stabilization. Much less attention has been devoted to induction of proper topography[51] (meant as the relative, cooperative arrangement of amino acid side chains) in peptides and proteins.

(48) Niccolai, N.; Garsky, V.; Gibbons, W. A. *J. Am. Chem. Soc.* **1980**, *102*, 1517–1520.
(49) Niccolai, N.; Schnoes, H. K.; Gibbons, W. A. *J. Am. Chem. Soc.* **1980**, *102*, 1513–1517.
(50) Hruby, V. J. *Life Sci.* **1982**, *31*, 189–199.
(51) Hruby, V. J.; Al-Obeidi, F.; Kazmierski, W. *Biochem. J.* **1990**, *268*, 249–262.
(52) Toniolo, C. *Int. J. Pept. Protein Res.* **1990**, *35*, 287–300.
(53) Mutter, M.; Hersperger, R.; Gubernator, K.; Muller, K. *Proteins* **1989**, *5*, 13–21.
(54) Seebach, D.; Aebi, J. D.; Naef, R.; Weber, T. *Helv. Chim. Acta* **1985**, *68*, 144–154.
(55) Bonora, G. M.; Toniolo, C.; Di Blascio, B.; Pavonie, C.; Benedetti, E.; Lingham, I.; Hardy, P. *J. Am. Chem. Soc.* **1984**, *106*, 8152–8156.
(56) Feigel, M. *J. Am. Chem. Soc.* **1986**, *108*, 181–182.
(57) Kemp, D. S.; Carter, J. S. *J. Org. Chem.* **1989**, *54*, 109–115, and references therein.
(58) Gierasch, L. M.; Deber, C. M.; Madison, V.; Niu, C.-H.; Blout, E. R. *Biochemistry* **1981**, *20*, 4730–4738.

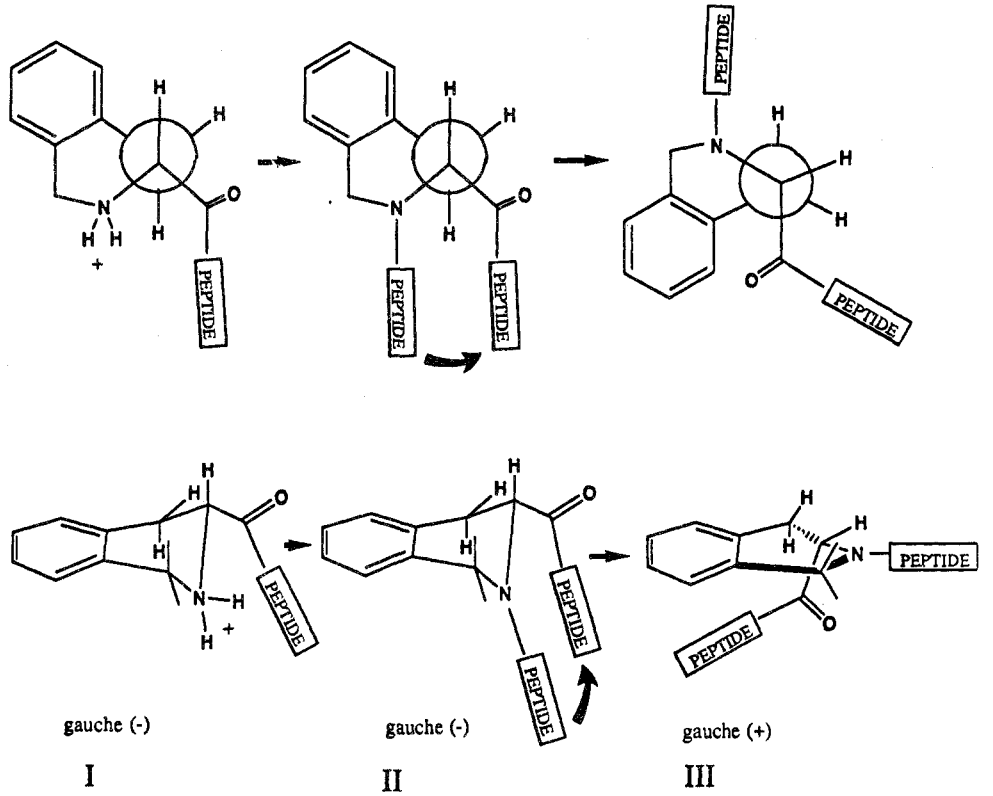

Figure 3. Conformational transformations of D-1,2,3,4-tetrahydroisoquinoline-3-carboxylic acid (D-Tic). Newman projections (upper drawing) correspond to the bottom level figures (within the same column). I. D-Tic with free amino group prefers gauche (−) side-chain conformation. II. Peptide chain attachment on N termini of D-Tic causes 1,2 pseudoequatorial strains (bent arrows) destabilizing the gauche (−) conformation. III. The heterocyclic ring flips to a gauche (+) side chain conformation, in which both the N and C substituents bear a 1,2 pseudoaxial relationship devoid of strains.

When the design involves primarily constraint of the side-chain moieties of a peptide or protein that has a well-defined backbone conformation, we propose the term "topographical design on stable templates". In the cases illustrated in this paper, aromatic side chains have been biased or frozen to a particular side-chain conformation by using 1,2,3,4-tetrahydroisoquinolinecarboxylic acid (Tic), which possesses a gauche (−) conformation for Tic when it is the N-terminal residue, and gauche (+) when the residue is incorporated internally (Figure 3). The gauche (+) conformation is usually the least stable for most amino acids. In any case, the configurational change results in two strongly repulsive gauche interactions between the β and N, as well as the β and C substituents, whereas the generally more stable gauche (−) conformation (as for D-Tic in peptide **2**[22]) shows only a single gauchelike relationship of substituents around the C–C bond (Figure 3). This conformational behavior of D-Tic in **2** can be explained by the concept of pseudoallylic strains,[59] in which tetrahydroisoquinolinecarboxylic acid in the N-terminal position of a peptide sequence prefers the gauche (−) conformation (Figure 3). When an amino acid is coupled to the amino function of Tic (e.g., Gly in **3**) so that the Tic residue now occupies an internal position in the peptide, a change of amine nitrogen hybridization from sp^3 to a partial sp^2 results in strong 1,2 diequatorial repulsive interactions between the N and C substituents (Gly and Cys, respectively) of the Tic amino acid (Figure 3). This highly energetic configuration, II, is unstable and undergoes a ring inversion to the conformation III (Figure 3), in which the N and C substituents are in a 1,2 diaxial relationship. This rearrangement forces the pipecolic acid ring to a gauche (+) conformation about the χ_1 angle. The increased stability of the gauche (+) form is due to replacement of strong 1,2 diequatorial repulsions by weak 1,2 diaxial interactions. The dramatic differences in the specific chemical shifts in peptides **2** and **3** are completely consistent with the proposed side-chain conformational change in the D-Tic residue. Similar extension can be transferred into other aromatic amino acids including histidine,[60] tyrosine, and tryptophan.[61]

The transverse and longitudinal relaxation rate studies on peptides **1–4**, allowed us to determine the critical interproton distances in these molecules and have shown here that a Tic residue does not distort the backbone conformation. Since the conformation in the 20-membered disulfide-containing ring remains a type II′ β turn in all cases, the overall topography of the peptide can be manipulated in such a way as to examine the possible "bioactive" one, as in peptide **2** (Figure 1, Figure 2B).

In principle, this approach allows one to probe the importance of specific surface structural elements for recognition and binding to the host receptor molecules. In the examples examined here, rotation of aromatic residues (due to their gauche (+) conformation) in the first and third position in **3** and **4**, respectively, to the opposite side of molecules resulted in a change in the topographical properties of the peptide. Biologically, a sharp decrease in receptor binding resulted, suggesting that these aromatic rings may in fact constitute important sites of interaction with the μ opioid receptor Figure 2c and d, respectively).

In addition, the gauche (−) side-chain conformation of D-Tic[1] in **2** places this aromatic ring further away from another pharmacophore, the Tyr[3]. In comparison with D-Phe[1] (staggered rotamers) and Tyr[3] in parent peptide **1**, this topographical modification is paralleled by an increased μ opioid receptor affinity and selectivity for **2** (Table I). This suggests a bioactive model of μ opioid receptor ligands in which the aromatic ring pharmacophores in positions 1 and 3 are some distance from one another.

Recently Hruby et al.,[62] on the basis of a combined approach involving ^{1}H NMR and molecular dynamics of the potent δ opioid receptor selective peptide Tyr-D-Pen-Gly-Phe-D-Pen (DPDPE), suggested a bioactive conformation in which both aromatic rings are on the same face in fairly close proximity, rendering the

(59) Johnson, F. *Chem. Rev.* **1968**, *68*, 375–413.

(60) Zechel, C.; Trivedi, D.; Hruby, V. J., manuscript submitted.
(61) Kazmierski, W. Ph.D. Thesis, University of Arizona, 1988.
(62) Hruby, V. J.; Kao, L.-F.; Pettitt, B. M.; Karplus, M. *J. Am. Chem. Soc.* **1988**, *110*, 3351–3359.

molecule amphiphilic. Our results presented here indicate that whereas the topographical proximity of the Tyr[1] and Phe[4] aromatic rings in DPDPE and the overall amphiphilic properties of the peptide may be critical for interaction with the δ receptor, the μ opioid receptors seem to bind ligands with significant separation of the aromatic (e.g., [D-Tic[1]]CTP (**2**)).

Further efforts in our laboratory are concentrated on design and synthesis of amino acids with constrained conformational properties that are complimentary to these already exhibited by 1,2,3,4-tetrahydroisoquinolinecarboxylate derivatives.

Acknowledgment. This research was supported by a grant from the National Science Foundation DMB-8712133 and by U.S. Public Health Service Grant NS 19972. We thank Prof. Dr. W. F. van Gunsteren and Prof. Dr. H. T. C. Berendsen (University of Groningen) for their GROMOS software package. We thank Ms. Susan Yamamura (computer graphics facilities) and Dr. Kenner Christiansen (NMR) for their kind assistance. FTNMR version 5.1 was obtained from Dr. D. Hare (Hare Research, Inc.). The Midwest Center for Mass Spectrometry is acknowledged for FAB-MS spectra of peptides **1-4** (NSF Regional Instrumentation Facility, Grant CHE 8211164).

Registry No. 1, 103335-28-0; **2**, 115981-69-6; **3**, 115962-17-9; **4**, 131904-39-7; Boc-Thr(*O*-Bzl), 15260-10-3; Boc-Pen(*S*-4-MeBzl), 104323-41-3; Boc-Orn(*N*-Cbz), 2480-93-5; Boc-D-Trp, 5241-64-5; Boc-Tic, 78879-20-6; Boc-Cys(*S*-4-MeBzl), 61925-77-7; Boc-D-Phe, 18942-49-9; Boc-D-Tic, 115962-35-1.

Supplementary Material Available: Full sets of data on the transverse and longitudinal cross-relaxation rates ($\sigma_\perp$, $\sigma_\parallel$), internuclear distances (r^{ij}), and correlation times (τ_c) for peptides **1-4**, stereoviews of the conformations derived from the methods discussed for 1, *3*, and *4*, and plots of the normalized (using eqs 4 and 5—see text) cross-peak intensities vs mixing times or spin-lock times in longitudinal and cross-relaxation experiments (11 pages). Ordering information is given on any current masthead page.

Contributions of Thiolate "Desolvation" to Catalysis by Glutathione *S*-Transferase Isozymes 1-1 and 2-2: Evidence from Kinetic Solvent Isotope Effects

Su-Er W. Huskey,*,† W. Phillip Huskey,*,‡ and Anthony Y. H. Lu†

Contribution from the Department of Animal and Exploratory Drug Metabolism, Merck Sharp and Dohme Research Labs, Rahway, New Jersey 07065, and Department of Chemistry, Rutgers, The State University, Newark, New Jersey 07102. *Received June 19, 1990*

Abstract: Kinetic solvent isotope effects on the reaction of glutathione with 1-chloro-2,4-dinitrobenzene catalyzed by rat liver glutathione *S*-transferase isozymes 1-1 and 2-2 (as expressed in Escherichia *coli*) have been measured. At pH (and pD) = 8.0, the isotope effects (H_2O/D_2O) ranged from 0.79 to 1.05 under various conditions of substrate concentrations. Solvent isotope effects were also measured for the nonenzymic reactions of glutathione or dithiothreitol with 1-chloro-2,4-dinitrobenzene. For reactions with the respective thiolate anions, solvent isotope effects of 0.84 and 0.87 were observed. For both the enzymic and nonenzymic reactions, the solvent isotope effects were interpreted in terms of hydrogen bond changes about the thiolate anion.

As catalysts for the nucleophilic addition of glutathione to a variety of electrophilic aromatic compounds, the glutathione *S*-transferases (EC 2.5.1.18) play an important role in the metabolism of endogenous and xenobiotic compounds.[1] The purification of individual isozymes has been complicated by the complexities of multiple forms (the enzymes exist as homo- or heterodimers[2]) and their microheterogeneities.[3] However, recent developments in molecular biology have made it possible to express cDNA of several glutathione transferase isozymes in *Escherichia coli* and make available large amounts of the enzyme for detailed mechanistic studies.[4]

Armstrong et al.[5] have studied the mechanisms of isozymes 3-3 and 4-4 in detail. Substantial evidence has been accumulated suggesting that these enzymes bind the protonated form of glutathione (referring to the thiol function), and that the anionic form is generated on the enzyme in the catalytic mechanism. Direct evidence has also been found for the formation of a Meisenheimer complex in the reaction of enzyme-bound glutathione anion with 1,3,5-trinitrobenzene.[5c] Substituent effects on rates measured with substituted chlorobenzenes and leaving-group effects are consistent with rate-limiting C-S bond formation for k_{cat}. An important feature[5a] of the mechanism is the apparent increase in the acidity of glutathione bound to the enzyme by roughly 2 pK_a units.

Scheme I

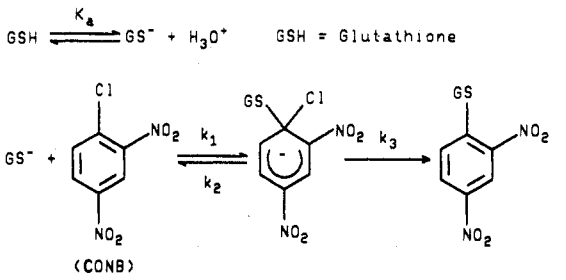

We suspected that the factors associated with the pK_a shift might involve stabilization of the anionic form of enzyme-bound

† Merck Sharp & Dohme Research Labs.
‡ Rutgers, The State University.

(1) (a) Jakoby, W. B. *Adv. Enzymol. Relat. Areas Mol. Biol.* **1978**, *46*, 383-414. (b) Mannervik, B. *Adv. Enzymol. Relat. Areas Mol. Biol.* **1985**, *57*, 357-417. (c) Armstrong, R. N. *CRC Crit. Rev. Biochem.* **1987**, *22*, 39-88. (d) Pickett, C. B.; Lu, A. Y. H. *Annu. Rev. Biochem.* **1989**, *58*, 743-764.
(2) Jakoby, W. B.; Ketterer, B.; Mannervik, B. *Biochem. Pharmacol.* **1984**, *33*, 2539-2540.
(3) (a) Pickett, C. B.; Telakowski-Hopkins, C. A.; Ding, G. J. F.; Argenbright, L.; Lu, A. Y. H. *J. Biol. Chem.* **1984**, *259*, 5182-5188. (b) Lai, H. C. J.; Li, N.; Weiss, M. J.; Reddy, C. C.; Tu, C. P. D. *J. Biol. Chem.* **1984**, *259*, 5536-5542. (c) Rothkopf, G. S.; Telakowski-Hopkins, C. A.; Stotish, R. L.; Pickett, C. B. *Biochemistry* **1986**, *25*, 993-1002. (d) Wang, I. Y.; Tung, E.; Wang, A.; Argenbright, L.; Wang, R. W.; Pickett, C. B.; Lu, A. Y. H. *Arch. Biochem. Biophys.* **1986**, *245*, 543-547.

0002-7863/91/1513-2283$02.50/0